Helsinki University of Technology Institute of Mathematics Research Reports

Espoo 2009 A564

BEST BILINEAR SHELL ELEMENT: FLAT, TWISTED OR CURVED?

Antti H. Niemi

TEKNILLINEN KORKEAKOULU
TEKNISKA HÖGSKOLAN
HELSINKI UNIVERSITY OF TECHNOLOGY
TECHNISCHE UNIVERSITÄT HELSINKI
UNIVERSITE DE TECHNOLOGIE D'HELSINKI

Helsinki University of Technology Institute of Mathematics Research Reports
Espoo 2009 A564

BEST BILINEAR SHELL ELEMENT: FLAT, TWISTED OR CURVED?

Antti H. Niemi

Dissertation for the degree of Doctor of Science in Technology to be presented, with due permission of the Faculty of Information and Natural Sciences, for public examination and debate in auditorium E at Helsinki University of Technology (Espoo, Finland) on the 27th of March 2009, at 12 o'clock noon.

Helsinki University of Technology
Faculty of Information and Natural Sciences
Department of Mathematics and Systems Analysis

Antti H. Niemi
Department of Mathematics and Systems Analysis
Helsinki University of Technology
P.O. Box 1100, FI-02015 TKK, Finland
E-mail: antti.h.niemi@tkk.fi

ISBN 978-951-22-9783-2 (print)
ISBN 978-951-22-9784-9 (PDF)
ISSN 0784-3143 (print)
ISSN 1797-5867 (PDF)
Multiprint Oy
Espoo 2009

Helsinki University of Technology
Faculty of Information and Natural Sciences
Department of Mathematics and Systems Analysis
P.O. Box 1100, FI-02015 TKK, Finland
email: math@tkk.fi http://math.tkk.fi/

Antti H. Niemi: *Best bilinear shell element: flat, twisted or curved?*; Helsinki University of Technology Institute of Mathematics Research Reports A564 (2009).

Abstract: This thesis concerns the accuracy of finite element models for shell structures. The focus is on low-order approximations of layer and vibration modes in shell deformations with particular reference to problems with concentrated loads. It is shown that parametric error amplification, or numerical locking, arises in these cases when bilinear elements are used and the formulation is based on the so-called degenerated solid approach. Furthermore, an alternative way for designing bilinear shell elements is discussed. The procedure is based on a refined shallow shell model which allows for an effective coupling between the membrane and bending strain in the energy expression.

AMS subject classifications: 74S05, 74K25

Keywords: shell elements, locking, shell layers, shell vibration modes, asymptotic behavior

Antti H. Niemi: *Paras bilineaarinen kuorielementti: tasainen, kiero vai kaareva?*

Tiivistelmä: Väitöskirjassa tarkastellaan kuorirakenteiden elementtiapproksimaatioiden tarkkuutta. Tutkimuksen kohteena on kuoren muodonmuutoksissa ilmenevien reunahäiriö- ja ominaisvärähtelymoodien mallinnus matalaasteisilla elementeillä. Työssä näytetään, että näiden approksimoinnissa esiintyy kuoren paksuusparametrista riippuvaa virheen vahvistumista eli numeerista lukkiutumista, mikäli laskennassa käytetään kahdeksansolmuisista tiilielementeistä degeneroituja nelisolmuisia bilineaarielementtejä. Työssä esitellään lisäksi vaihtoehtoinen tapa nelisolmuisen kuorielementin muodostamiseksi. Menettely perustuu hienostuneeseen matalan kuoren malliin, joka mahdollistaa kalvo- ja taipumavenymien tehokkaan kytkennän kuoren venymäenergian lausekkeessa.

Avainsanat: kuorielementit, lukkiutuminen, kuoren reunahäiriöt, kuoren värähtelymoodit, asymptoottinen käytös

Preface

This dissertation has been written at the Institute of Mathematics of the Helsinki University of Technology during the years 2005–2008. It consists of an overview, four published articles and one research report. The main sponsors of the project have been the Finnish National Graduate School in Engineering Mechanics and the Emil Aaltonen's Foundation.

I am most grateful to my supervisor Prof. Juhani Pitkäranta for sharing his wisdom regarding not only the shell problem but the academic world in general. I have also had many inspirational discussions with my other collaborator Dr. Harri Hakula for instance on the themes of numerical analysis and parenting. Then I would like to thank all my colleagues at the Institute of Mathematics, in particular the closest ones within the Finite Element Research Group, for creating a nice working environment.

It has been an honour to have Dr. Lourenço Beirão da Veiga from the University of Milan and Dr. Mika Malinen from CSC – IT Center for Science, two experts in the field, as the preliminary examiners of the thesis. In addition, thanks are due to the anonymous reviewers of the journal articles for their valuable comments and criticism that, I believe, have improved the thesis notably.

Finally, I acknowledge my parents for securing a comfortable childhood home, my brother for being a backup on many occasions, and especially my wife Elina and daughter Alisa for their love and support.

Espoo, February 2009 Antti H. Niemi

List of included publications

[A] A.H. Niemi, J. Pitkäranta, H. Hakula, Benchmark computations on point-loaded shallow shells: Fourier vs. FEM, *Computer Methods in Applied Mechanics and Engineering* 196 (2007), 894–907.

[B] A.H. Niemi, J. Pitkäranta, Bilinear finite elements for shells: Isoparametric quadrilaterals, *International Journal for Numerical Methods in Engineering* 75 (2008), 212–240.

[C] A.H. Niemi, Approximation of shell layers using bilinear elements on anisotropically refined rectangular meshes, *Computer Methods in Applied Mechanics and Engineering* 197 (2008), 3964–3975.

[D] A.H. Niemi, J. Pitkäranta, H. Hakula, Point load on a shell, In: *Numerical Mathematics and Advanced Applications*, K. Kunisch, G. Of, O. Steinbach (eds.), Springer, 2008, 819–826.

[E] A.H. Niemi, A bilinear shell element based on a refined shallow shell model, Helsinki University of Technology Institute of Mathematics Research Reports, A562 (2008), 30 pages. Submitted to *International Journal for Numerical Methods in Engineering*.

Author's contribution

Concerning papers [A], [B] and [D], the author of the thesis is responsible of the writing and substantial part of the analysis. In papers [A] and [D], the numerical results involving high-order finite elements were obtained using a computer code made by Harri Hakula.

Contents

1 Introduction **9**

2 Numerical approach to the shell problem **10**
2.1 Refined shallow shell model 12
2.2 Membrane and shear constraints, MITC4S 14
2.3 Bilinear degenerated 3D FEM, MITC4F 17
2.4 Case study: Vibration analysis of a fan blade 22

3 Concluding remarks **24**

References **25**

Included publications

1 Introduction

In the theory of elasticity, bodies which are bounded by two closely-spaced curved surfaces are referred to as shells. Because such structures support external loads very effectively, they are applied widely especially in naval and aerospace engineering where the combination of light weight and high strength is of uttermost importance. But thin elastic shells are rather common in nature as well. For instance, biomechanical models of artery walls in the human cardiovascular system are receiving a great deal of attention at the present time.

Since the equations of elasticity specialized to thin curved bodies cannot be solved analytically in general, practical shell problems are usually solved numerically by the finite element method. The exponential growth in raw computer power during the last decades has enabled structural engineers to address very complex problems with many interacting effects. Nevertheless, modeling of thin-walled structures with three-dimensional continuum elements would require several elements through the thickness and might lead to fairly expensive computations particularly when nonlinear and transient analyses are performed, cf. [1]. Therefore, special structural elements known as "shell elements" are often preferred in engineering applications. Among these, certain low-order formulations based on the so-called degenerated solid approach seem to be the most popular ones thanks to their relative simplicity and excellent performance in many benchmark problems, see e.g. [2, 3, 4, 5]. Rather paradoxically, the mathematical understanding of parametric locking effects within these formulations is still fairly light albeit the "underlying mathematical model" of the discretizations has been identified and studied in several works, see [6, 7, 8, 9, 10] and the references therein.

The present thesis is a continuation of the earlier theory [11, 12, 13, 14] (see also [15]) concerning the bilinear MITC4 shell element introduced by Bathe and Dvorkin in [4, 16]. Our approach to MITC4 (and other bilinear degenerated elements) is based on a reformulation of the original 3D element in the context of a specific 2D shell model. This model was derived directly from the geometrically exact Reissner-Naghdi shell model by Malinen in [11, 12] and may be viewed as a refined variant of the shallow shell models found from the classical books on shell theory such as [17, 18, 19, 20, 21]. The model includes some geometric simplifications but it should be precise enough to study the accuracy of low-order finite element formulations where rather crude geometric approximations are being performed anyway. In fact, the *numerical* effect of the bilinear geometry representation involved in MITC4 can be unfolded adequately when the formulation is understood in this context [12]. Regarding the approximation of bending- and membrane dominated deformations of a shell, the finite element error analysis was performed by Havu and Pitkäranta in [13, 14].

This work completes the picture by analyzing the locking effects related to the various boundary and interior layer modes appearing in shell deformations [22]. Some of the obtained results apply to the approximation of

vibration modes as well since these modes involve locking effects similar in nature to those found when approximating layers [23]. Moreover, the thesis asserts that the usefulness of classical shell models is not limited to academic purposes only. On the contrary, the refined shallow shell model can be used as a solid basis for efficient and accurate computations using bilinear finite elements.

The next section serves as an extended introduction for the thesis and outlines the questions that will be addressed. A brief summary of the main results is presented in the last section.

2 Numerical approach to the shell problem

Consider an elastic body occupying a domain Ω in 3-space and deformable according to the laws of linear elasticity theory. Denote the displacements along the coordinates x_1, x_2, x_3 by u_1, u_2, u_3 and the corresponding displacement vector field by $\mathbf{u} = (u_1, u_2, u_3)$. The strain energy of the body is then proportional to the quadratic functional

$$\mathcal{A}(\mathbf{u}, \mathbf{u}) = \int_\Omega \boldsymbol{\sigma}(\mathbf{u}) : \boldsymbol{\varepsilon}(\mathbf{u}) \, \mathrm{d}\Omega \tag{1}$$

where $\boldsymbol{\sigma}$ is the stress tensor and $\boldsymbol{\varepsilon}$ is the strain tensor. Assuming homogeneous and isotropic material, the stress is related to the strain by the *material law of Hooke* as

$$\boldsymbol{\sigma} = \lambda \operatorname{tr}(\boldsymbol{\varepsilon}) \mathbf{I} + 2\mu\boldsymbol{\varepsilon} \tag{2}$$

Here λ, μ are the *Lamé parameters* of the material which are connected to the *Young modulus* E and *Poisson ratio* ν by

$$\lambda = \frac{E\nu}{(1+\nu)(1-2\nu)}, \quad \mu = \frac{E}{2(1+\nu)}$$

In a Cartesian coordinate system $(\bar{x}_1, \bar{x}_2, \bar{x}_3)$ the strain tensor is defined as the symmetric gradient, i.e.

$$\epsilon_{ij} = \frac{1}{2}\left(\frac{\partial \bar{u}_i}{\partial \bar{x}_j} + \frac{\partial \bar{u}_j}{\partial \bar{x}_i}\right) \tag{3}$$

but in the geometric description of a shell body it is more suitable to employ curvilinear coordinates[1].

More precisely, the position of any point in a shell may be determined by three coordinates x, y, z so that x and y specify the position on the middle surface, while z expresses the normal distance to the point from the middle surface. The middle surface is assumed to be a parametric surface $\mathbf{r}(x, y)$, where $\mathbf{r}$ is a smooth function that maps the parameter region $\omega \subset \mathbb{R}^2$ into 3-space. Denoting by $\mathbf{n}$ the unit normal vector to the middle surface, a shell

[1]This thesis relies on conventional notation in physical components, although more general tensor notation is often preferred in modern presentations of shell theory.

domain of constant thickness t can now be defined as $\Omega = \mathbf{\Phi}(\omega \times (-t/2, t/2))$, where $\mathbf{\Phi}$ is a smooth map of the form

$$\mathbf{\Phi}(x, y, z) = \mathbf{r}(x, y) + z\mathbf{n}(x, y) \tag{4}$$

In classical shell theories the displacement field $\mathbf{u} = (u_1, u_2, u_3)$ at a point (x, y, z) is defined so that u_1, u_2 are the *tangential* displacements to the middle surface and u_3 is the *normal* displacement. Moreover, the variation of the displacement field $\mathbf{u}$ with respect to the normal coordinate z is assumed to be of the form

$$\begin{aligned} u_1(x, y, z) &= u(x, y) - z\theta(x, y) \\ u_2(x, y, z) &= v(x, y) - z\psi(x, y) \\ u_3(x, y, z) &= w(x, y) \end{aligned} \tag{5}$$

where u, v and w are the displacements of the middle surface and θ and ψ are the so-called rotations. In other words, straight material fibres which are perpendicular to the middle surface before deformation remain straight after deformation and do not change their length. Nowadays, this assumption is probably best known as the *Reissner-Mindlin kinematic assumption*.

In addition, most of the classical shell models neglect the normal stress in comparison with the remaining stresses. Together with (2), the *plane stress assumption* $\sigma_{33} = 0$ implies that

$$\epsilon_{33} = -\frac{\nu}{1+\nu}(\epsilon_{11} + \epsilon_{22}) \tag{6}$$

Obviously this contradicts assumption (5) which already implies that $\epsilon_{33} = \partial u_3/\partial z = 0$. The conflict causes ultimately no problem, but a rigorous justification of the plane stress hypothesis is actually a rather delicate matter. The mathematical reasoning can be based on a quadratic expansion of u_3 in the normal coordinate z. As a matter of fact, the condition $\sigma_{33} = 0$ then follows (approximatively, see e.g. [24]) from the minimization of the 3D strain energy with respect to the linear and quadratic components in u_3.

Anyway, substitution of ϵ_{33} from (6) back to (2), (1) yields the 3D strain energy of a linear elastic problem with $\sigma_{33} = 0$ (homogeneous, isotropic material):

$$\begin{aligned} \mathcal{A}(\mathbf{u}, \mathbf{u}) = &\frac{E}{1-\nu^2} \int_\Omega \left[\nu(\epsilon_{11} + \epsilon_{22})^2 + (1-\nu)(\epsilon_{11}^2 + 2\epsilon_{12}^2 + \epsilon_{22}^2)\right] \, \mathrm{d}\Omega \\ &\frac{2E}{(1+\nu)} \int_\Omega \left(\epsilon_{13}^2 + \epsilon_{23}^2\right) \, \mathrm{d}\Omega \end{aligned} \tag{7}$$

Referring to the assumed expansion (5) of the displacement field, the remaining strains in the expression (7) can be put in the approximative form

$$\begin{aligned} \epsilon_{ij}(x, y, z) &= \beta_{ij}(x, y) - z\kappa_{ij}(x, y), \quad i, j = 1, 2, \\ 2\epsilon_{i3}(x, y, z) &= \rho_i(x, y), \quad i = 1, 2 \end{aligned}$$

Here β_{ij} are referred to as the *membrane strains*, κ_{ij} as the *bending strains* and ρ_i as the *transverse shear strains*. These are in general variable-coefficient

linear combinations of the displacement components u, v, w, θ, ψ and their first-order partial derivatives with respect to x, y. The actual form of the coefficients depends on how the coordinates x, y have been chosen, but when the coordinate lines are orthogonal, the coefficients can be written (see [19]) in terms of the two *Lamé parameters*[2]

$$A_1 = \left|\frac{\partial \mathbf{r}}{\partial x}\right|, \quad A_2 = \left|\frac{\partial \mathbf{r}}{\partial y}\right|$$

and the three *radii of curvature*[3]

$$\frac{1}{R_{11}} = -\frac{1}{A_1^2}\mathbf{n} \cdot \frac{\partial^2 \mathbf{r}}{\partial x^2}, \quad \frac{1}{R_{22}} = -\frac{1}{A_2^2}\mathbf{n} \cdot \frac{\partial^2 \mathbf{r}}{\partial y^2}, \quad \frac{1}{R_{12}} = -\frac{1}{A_1 A_2}\mathbf{n} \cdot \frac{\partial^2 \mathbf{r}}{\partial x \partial y}$$

The quantities A_1 and A_2 (also referred to as scale factors) determine the differential of the arc length on the middle surface by

$$ds^2 = A_1^2 dx^2 + A_2^2 dy^2$$

whereas the quantities $1/R_{11}$ and $1/R_{22}$ represent the normal curvatures of the middle surface along the coordinate lines. The geometric depiction of the twist $1/R_{12}$ is more complex, but it can be related to the *principal curvatures* $1/R_1$ and $1/R_2$, from which one is the maximum and the other one a minimum of the normal curvature, as

$$\frac{1}{R_{12}} = \left(\frac{1}{R_2} - \frac{1}{R_1}\right) \sin\alpha \cos\alpha$$

where α is the angle between the x-coordinate line and the direction of the principal curvature $1/R_1$.

2.1 Refined shallow shell model

In what follows, the coordinates x, y are identified as the projections of points of the shell's middle surface on a plane $K \leftrightarrow \omega \subset \mathbb{R}^2$ so that the middle surface may be represented as

$$\mathbf{r}(x, y) = x\mathbf{i} + y\mathbf{j} + f(x, y)\mathbf{k}, \quad (x, y) \in K \tag{8}$$

Here $\mathbf{i}, \mathbf{j}, \mathbf{k}$ are the basis vectors of the Cartesian coordinates $\bar{x}_1, \bar{x}_2, \bar{x}_3$ and f is a smooth function. Let us denote the smallest radius of curvature of $\mathbf{r}(x, y)$ over K by $R = \min\{R_{11}, R_{22}, R_{12}\}$ and the diameter of K by $h_K = \operatorname{diam}(K)$. We will assume that $|\boldsymbol{\nabla} f| = \mathcal{O}(h_K/R)$ which implicates that the plane K is (approximatively) tangent to the middle surface. It follows that

[2]Gabriel Lamé (1795–1870) made substantial contributions to both elasticity theory and general theory of curvilinear coordinates.

[3]We follow the usual convention in shell theory, where the normal curvature at a point $(x, y) \in \omega$ is positive when the corresponding center of curvature lies in the direction $-\mathbf{n}(x, y)$ from $\mathbf{r}(x, y)$.

the coordinate lines on the middle surface are orthogonal within the accuracy of $\mathcal{O}(h_K^2/R^2)$. Up to this accuracy, the scale factors may be written as

$$A_1 = \sqrt{1 + \left(\frac{\partial f}{\partial x}\right)^2} \approx 1, \quad A_2 = \sqrt{1 + \left(\frac{\partial f}{\partial y}\right)^2} \approx 1 \tag{9}$$

and the curvatures may be taken to be the second derivatives of f in (8), i.e.

$$\frac{1}{R_{11}} \approx \frac{\partial^2 f}{\partial x^2}, \quad \frac{1}{R_{22}} \approx \frac{\partial^2 f}{\partial y^2}, \quad \frac{1}{R_{12}} \approx \frac{\partial^2 f}{\partial x \partial y}$$

However, an attractive option is to compute these directly from the unit normal vector $\mathbf{n}$ as

$$\frac{1}{R_{11}} \approx \frac{\partial \mathbf{n}}{\partial x} \cdot \mathbf{i}, \quad \frac{1}{R_{22}} \approx \frac{\partial \mathbf{n}}{\partial y} \cdot \mathbf{j}, \quad \frac{1}{R_{12}} \approx \frac{\partial \mathbf{n}}{\partial x} \cdot \mathbf{j} \approx \frac{\partial \mathbf{n}}{\partial y} \cdot \mathbf{i} \tag{10}$$

The strain-displacement[4] relations over K can now be written for the membrane strains as

$$\beta_{11} = \frac{\partial u}{\partial x} + \frac{w}{R_{11}}, \quad \beta_{22} = \frac{\partial v}{\partial y} + \frac{w}{R_{22}}, \quad \beta_{12} = \frac{1}{2}\left(\frac{\partial u}{\partial y} + \frac{\partial v}{\partial y}\right) + \frac{w}{R_{12}} \tag{11}$$

for the transverse shear strains as

$$\rho_1 = \theta - \frac{\partial w}{\partial x} + \frac{u}{R_{11}} + \frac{v}{R_{12}}, \quad \rho_2 = \psi - \frac{\partial w}{\partial y} + \frac{u}{R_{12}} + \frac{v}{R_{22}} \tag{12}$$

and for the bending strains as

$$\begin{aligned} \kappa_{11} &= \frac{\partial \theta}{\partial x} + \frac{1}{2}\frac{1}{R_{12}}\left(\frac{\partial u}{\partial y} - \frac{\partial v}{\partial x}\right), \quad \kappa_{22} = \frac{\partial \psi}{\partial y} - \frac{1}{2}\frac{1}{R_{12}}\left(\frac{\partial u}{\partial y} - \frac{\partial v}{\partial x}\right) \\ \kappa_{12} &= \frac{1}{2}\left[\frac{\partial \theta}{\partial y} + \frac{\partial \psi}{\partial y} - \frac{1}{R_{11}}\left(\frac{\partial u}{\partial y} - \frac{w}{R_{12}}\right) - \frac{1}{R_{22}}\left(\frac{\partial v}{\partial x} - \frac{w}{R_{12}}\right)\right] \end{aligned} \tag{13}$$

where the curvatures $1/R_{ij}$ are the only visible geometric parameters. The above forms have been obtained by admitting a truncation error of $\mathcal{O}(h_K/R)$ which arises from the substitution of (9) into the usual 2D strain expressions as given by Gol'denveizer in [19, Eqs. (19.1)–(19.5)].

By writing $\mathrm{d}\Omega = \mathrm{d}x\,\mathrm{d}y\,\mathrm{d}z$, the three-dimensional deformation energy (7) may be integrated over z within the adopted accuracy . The resulting two-dimensional strain energy functional of the shell over K takes the form

$$\begin{aligned} \mathcal{A}_K(\mathbf{u},\mathbf{u}) =& \frac{Et}{1-\nu^2}\int_K \left[\nu(\beta_{11}+\beta_{22})^2 + (1-\nu)(\beta_{11}^2 + 2\beta_{12}^2 + \beta_{22}^2)\right]\,\mathrm{d}x\mathrm{d}y \\ &+ \frac{Et}{2(1+\nu)}\int_K \left[\rho_1^2 + \rho_2^2\right]\,\mathrm{d}x\mathrm{d}y \\ &+ \frac{Et^3}{12(1-\nu^2)}\int_K \left[\nu(\kappa_{11}+\kappa_{22})^2 + (1-\nu)(\kappa_{11}^2 + 2\kappa_{12}^2 + \kappa_{22}^2)\right]\,\mathrm{d}x\mathrm{d}y \end{aligned} \tag{14}$$

[4]Note that here the displacement components do not follow the coordinate axes $\bar{x}_1, \bar{x}_2, \bar{x}_3$, but are *tangents* to the middle surface in planes parallel to the coordinate planes (u, v, θ, ψ) and *normal* to the middle surface (w).

The shell model (11)–(14) whose derivation is outlined above serves as the starting point of our study. The model was originally presented by Malinen in [12] using general coordinates and tensorial notation. Actually the bending strains proposed in [12] differ from the ones in (13) by the relations

$$\kappa_{11}^M = \kappa_{11} - \frac{1}{R_{12}}\beta_{12}, \quad \kappa_{22}^M = \kappa_{22} - \frac{1}{R_{12}}\beta_{12}$$

but like any modification of the bending strains by an added linear combination of β_{ij}'s, this causes an insignificant perturbation of the energy (14) when t is small. On the other hand, the effect of the tangential displacements u and v in the expressions of the bending strains is neglected completely in the classical engineering theory of shells (also known as the Donnell-Musthari-Vlasov theory of thin shells, see [21]). From the modern perspective, this type of simplification is reasonable e.g. when the goal is to understand locking of finite element algorithms because the bending strains are not so critical in this respect.

However, when the model is used in realistic computations to represent the strain energy of a single element K, there are generally two possibilities as, according to [22], the omission of the middle surface displacements from (13) effectively attaches the displacement component w to the $\mathbf{k}$-direction. Either all terms in the expression (13) are retained or the direction of the third displacement component is defined differently within each element. In any event, the strain energy of the entire shell may be expressed formally as

$$\mathcal{A}(\mathbf{u}, \mathbf{u}) = \sum_K \mathcal{A}_K(\mathbf{u}, \mathbf{u})$$

where the sum is taken over all elements used in the representation of the structure.

2.2 Membrane and shear constraints, MITC4S

The difficulties in linear shell finite element models originate mainly in the approximation of inextensional deformations with vanishing membrane and transverse shear strains. Such deformations may occur when the kinematic constraints along the edge of the shell are weak enough to allow pure bending of the curved structure. To illustrate the problems with the associated displacement modes, we consider a simple example in the spirit of [25].

Assume a four-node isoparametric quadrilateral element occupying a rectangular domain aligned with the coordinate axes x, y. The element expansions of u and w take then the bilinear form

$$u(x, y) = \alpha_u + \beta_u x + \gamma_u y + \delta_u xy, \quad w(x, y) = \alpha_w + \beta_w x + \gamma_w y + \delta_w xy$$

where the constants α_u, β_u, etc. depend on the values of u and w at the element nodes. The requirement $\beta_{11} = 0$ implies according to (11) that

$$\left(\beta_u + \frac{\alpha_w}{R_{11}}\right) + \frac{\beta_w}{R_{11}}x + \left(\delta_u + \frac{\gamma_w}{R_{11}}\right) y + \frac{\delta_w}{R_{11}}xy = 0$$

so that four constraints are imposed on u and w. In particular, w is not allowed to vary with respect to x which is a rather heavy requirement from the viewpoint of approximation theory. Moreover, each of the conditions $\beta_{12} = \beta_{22} = 0$ and $\rho_1 = \rho_2 = 0$ satisfied by an inextensional deformation restricts the bilinear displacement field with additional four constraints. Note that when the element is a part of a large rectangular mesh, it has approximatively one degree of freedom per displacement component[5]. In other words, the element is heavily over-constrained which results in a severe underestimation of the displacements, or locking, see [24].

As a quick device for estimating an element's tendency to over-stiffness, Hughes has introduced the so-called *constraint ratio*

$$r = \frac{N_{\text{eq}}}{N_{\text{c}}} \tag{15}$$

where N_{eq} is the total number of discrete equilibrium equations and N_{c} is the total number of harmful constraints, see [25]. Ideally, the value of r should approach r_{ideal}, the ratio of equilibrium equations to constraints for the continuous problem, as the mesh is refined. If $r < r_{\text{ideal}}$, locking is expected, whereas $r > r_{\text{ideal}}$ might indicate that the element is too flexible. In our case the ideal value is $r_{\text{ideal}} = \frac{5}{5} = 1$ while for the bilinear element we have $r = \frac{5}{20} = 0.25$.

We have seen that if the convenient bilinear interpolations for the displacements are to be used, some kind of reduction of constraints is necessary in order to suppress the locking effect. In mathematical terms, such reduction can be carried out in many ways like by using strain projections (assumed strain approach) or by resorting to mixed methods where the membrane and transverse shear stresses are approximated as independent unknowns. The schemes become unavoidably rather elaborate for isoparametric elements of irregular shape, but there exists a canonical projection rule valid for rectangular elements which we shall describe next. In the thesis, this formulation is referred to as MITC4S because of its close relation with the MITC4 shell element used in actual engineering computations.

The procedure begins with evaluation of the components of membrane and transverse shear strains tangent to each of the element's four edges at the midpoint of the edge in question. In other words, the components β_{11}, ρ_1 are evaluated at the midpoints of the horizontal edges and the components β_{22}, ρ_2 are evaluated at the midpoints of the vertical edges. Moreover, the membrane shear strain β_{12} is evaluated at the center of the element, see Figure 1. The nine values so obtained are then used to determine the constants $c_1, \ldots, c_9$ in the expressions

$$\boldsymbol{\beta}_h = \begin{bmatrix} c_1 + c_2 y & c_5 \\ c_5 & c_3 + c_4 x \end{bmatrix}, \quad \boldsymbol{\rho}_h = \begin{bmatrix} c_6 + c_7 y \\ c_8 + c_9 x \end{bmatrix} \tag{16}$$

[5]For a $N \times N$ mesh of rectangular elements, the ratio of number of nodes to number of elements approaches unity as $N \to \infty$ because $\lim_{N\to\infty} \frac{(N+1)^2}{N^2} = 1$

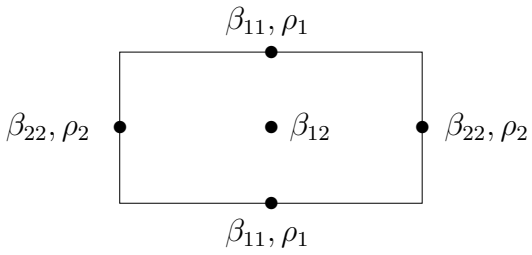

Figure 1: The evaluation points for the membrane and the transverse shear strains in the projection rule.

Accordingly, on a large rectangular mesh we will have two constraints per each side and one constraint per each element, i.e. five constraints per element on average[6] so that $r = 1$, the ideal value. In addition, the weakened constraints may be viewed as straightforward finite difference approximations of the corresponding constraints arising from the continuous problem. For instance, the condition $\beta_{11,h} = 0$ written in terms of the (global) nodal displacement degrees of freedom reads

$$\frac{u(x_{i+1}, y_j) - u(x_i, y_j)}{x_{i+1} - x_i} + \frac{1}{2R_{11}(x_{i+1/2}, y_j)}(w(x_{i+1}, y_j) + w(x_i, y_j)) = 0$$

which turns out to be a second order scheme with respect to x for the equation $\partial u/\partial x + w/R_{11} = 0$. The complete 5×5 system which arises in the approximation of bending-dominated deformations has been analyzed under strong assumptions about the geometry of the problem by Havu and Pitkäranta in [13].

On the other hand, the use of $\beta_{ij,h}$ in place of β_{ij} breaks the Rayleigh-Ritz code obeyed by standard finite elements, cf. [26]. The violation, which arises locally in the computation of the strain energy (14), requires careful analysis of the consistency error functional

$$\mathcal{A}(\mathbf{u}, \mathbf{v}) - \mathcal{A}_h(\mathbf{u}, \mathbf{v}) = \delta_h(\mathbf{v}) \tag{17}$$

especially when the displacement field $\mathbf{u}$ to be approximated is not bending-dominated. Note that here $\mathbf{v}$ denotes an arbitrary trial function from the finite element space where the kinematic constraints of the problem have been replaced by their homogeneous versions (see e.g. [27] for more details). Concerning membrane-dominated deformations, i.e. situations where pure bending of the shell is prevented for instance by kinematic constraints, sharp bounds for the consistency error functional have been derived in [14], but again under rather strong assumptions about the problem set-up.

[6]For a $N \times N$ mesh of rectangular elements, the ratio of number of nodes to number of sides approaches one half as $N \to \infty$ because $\lim_{N\to\infty} \frac{(N+1)^2}{2N(N+1)} = \frac{1}{2}$.

The analysis in [13, 14] left open two questions in particular. Firstly, the ability of MITC4S to capture boundary and interior layers was not addressed in these works. Secondly, the necessity of the highly specific assumptions made in the error analysis remained unclear. These questions have been answered to some extent in papers [A] and [B] of this thesis.

Paper [A] begins our study on the approximation of shell layers by introducing a set of academic model problems where the shell is under a concentrated point load. In the paper, the problem set was solved by MITC4S along with standard (i.e. no projection rule is applied whatsoever) high-order finite finite elements and the results were compared with analytical reference solutions. Note that while point loads are not admissible in the variational sense within the Reissner-Mindlin framework, they are anyway rather common in engineering practice. Point loads ought not to be overlooked by mathematicians either because the corresponding solution represents the Green's function for the problem.

Nevertheless, layers and concentrated loads are left in the background in paper [B] where the reduced strain scheme is investigated under more general circumstances. First of all, the paper examines different extensions of the above projection rule so as to allow more general quadrilateral element shapes. The performance of the alternative formulations was then evaluated in both membrane- and bending-dominated problems with different shell geometries. The dual nature of the problem become very clear in the work as, on a general mesh, it turned out to be very difficult to obtain a reasonable bound for the consistency error functional (17) in membrane-dominated deformations and circumvent the locking effect in bending-dominated deformations at the same time.

The rest of the thesis concentrates again on the layer problem. The motivation for this comes from certain differences between MITC4S and MITC4 that have been anticipated in [11, 12] where the inter-element connection was established in the first place. These differences will be highlighted in the following section.

2.3 Bilinear degenerated 3D FEM, MITC4F

The majority of shell finite elements used in engineering practice are *not* derived from 2D shell models basically because the mapping (4) defining the shell geometry is not readily available in computer-aided design programs. Instead, the geometric initial data consists of nodes located on the shell middle surface in conjunction with their associated unit normal vectors and thickness parameters, see e.g. [10]. The shell geometry is then approximated using isoparametric finite element techniques and the previously discussed kinematic and mechanical assumptions of the Reissner-Mindlin type are imposed in that context. This hinders numerical error analysis of such formulations, since the mathematical understanding of shell deformations is based predominantly on the geometrically exact 2D shell models. In particular, the question pertains to bilinear formulations where the geometry approxima-

tion involving straight-sided elements becomes rather crude. To see this, we follow [12] and examine how the leading terms of the usual two-dimensional strains are represented by bilinear degenerated elements.

For this purpose, we analyze a single element $\bar{K}$ which is thought to be given in terms of (4) and (8) by replacing f and $\mathbf{n}$ by their bilinear interpolants $\tilde{f}$ and $\tilde{\mathbf{n}}$, respectively[7]. In our notation, the Reissner-Mindlin kinematic assumption at a node i reads

$$\mathbf{u}_i = (u_i - z\theta_i)\mathbf{e}_1^{(i)} + (v_i - z\psi_i)\mathbf{e}_2^{(i)} + w_i\mathbf{e}_3^{(i)}$$

where $\mathbf{e}_3^{(i)} = \tilde{\mathbf{n}}(x_i, y_i)$ is the nodal director and $\mathbf{e}_1^{(i)}, \mathbf{e}_2^{(i)}$ are two orthogonal directions to it. Let us assume that these are constructed so that $\mathbf{e}_1^{(i)}$ and $\mathbf{e}_2^{(i)}$ are (approximatively) orthogonal to $\mathbf{j}$ and $\mathbf{i}$, respectively, so that $u_i, v_i, w_i, \theta_i, \psi_i$ can be regarded directly as the degrees of freedom for the geometrically compatible shell model of Section 2.1. Resolving $\mathbf{u}_i$ into components parallel to the directions $\mathbf{i}, \mathbf{j}, \mathbf{k}$ used in the geometry representation yields

$$\mathbf{u}_i = \bar{u}_i\mathbf{i} + \bar{v}_i\mathbf{j} + \bar{w}_i\mathbf{k}$$

where

$$\begin{aligned} \bar{u}_i &= u_i + w_i(\mathbf{e}_3^{(i)} \cdot \mathbf{i}) - z\theta_i \\ \bar{v}_i &= v_i + w_i(\mathbf{e}_3^{(i)} \cdot \mathbf{j}) - z\psi_i \\ \bar{w}_i &= w_i - u_i(\mathbf{e}_3^{(i)} \cdot \mathbf{i}) - v_i(\mathbf{e}_3^{(i)} \cdot \mathbf{j}) \end{aligned} \tag{18}$$

within the relative error of $\mathcal{O}(h_K^2/R^2)$.

Concerning the implementation of the plane stress hypothesis, we note that slightly different directions for which the stresses vanish have been proposed in the literature, see e.g. [28, 29]. Here, as in [12], the normal stress in the $\bar{x}_3$-direction will be neglected by using the assumption (6). Consequently, the strain energy functional takes then the form (7) where the rectangular Cartesian components of the strain tensor are given by (3):

$$\epsilon_{11} = \frac{\partial \bar{u}}{\partial \bar{x}_1}, \quad \epsilon_{22} = \frac{\partial \bar{v}}{\partial \bar{x}_2}, \quad \epsilon_{12} = \frac{1}{2}\left(\frac{\partial \bar{u}}{\partial \bar{x}_2} + \frac{\partial \bar{v}}{\partial \bar{x}_1}\right)$$

and

$$\epsilon_{13} = \frac{1}{2}\left(\frac{\partial \bar{u}}{\partial \bar{x}_3} + \frac{\partial \bar{w}}{\partial \bar{x}_1}\right), \quad \epsilon_{23} = \frac{1}{2}\left(\frac{\partial \bar{v}}{\partial \bar{x}_3} + \frac{\partial \bar{w}}{\partial \bar{x}_2}\right)$$

Still following [12], we define the corresponding membrane and bending strains of the approximative middle surface $\bar{x}_3 = \tilde{f}$ as

$$\bar{\beta}_{ij} = \epsilon_{ij}(\bar{x}_1, \bar{x}_2, \tilde{f}), \quad \bar{\kappa}_{ij} = -\frac{\partial \epsilon_{ij}}{\partial \bar{x}_3}(\bar{x}_1, \bar{x}_2, \tilde{f}) \quad i, j = 1, 2$$

and the transverse shear strains as

$$\bar{\rho}_i = 2\epsilon_{i3}(\bar{x}_1, \bar{x}_2, \tilde{f}), \quad i = 1, 2$$

[7]Note that when the four nodes of $\bar{K}$ are coplanar, $\tilde{f}$ may be taken to be identically zero.

Referring to the xyz-coordinate system we may write then

$$\bar{\beta}_{11} = \left.\frac{\partial \bar{u}}{\partial \bar{x}_1}\right|_{\bar{x}_3=\tilde{f}} = \left.\frac{\partial \bar{u}}{\partial x}\right|_{z=0} + \mathcal{O}(h_K/R) \tag{19}$$

Assume now that K is a rectangle so that the interpolated normal vector at a node (x_i, y_i) can be expanded as

$$\mathbf{e}_3^{(i)} = \tilde{\mathbf{n}}(0,0) + \frac{\partial \tilde{\mathbf{n}}}{\partial x}(x_i, y_i)x_i + \frac{\partial \tilde{\mathbf{n}}}{\partial y}(0,0)y_i, \quad i = 1,2,3,4$$

where the origin of the coordinates x, y coincides with the element center. Using this expansion together with (19), (18) and (10) yields

$$\bar{\beta}_{11} = \frac{\partial u}{\partial x} + \Pi_x\left(\frac{w}{R_{11}}\right) + \frac{R_y(w)}{R_{12}(0,0)} \tag{20}$$

where Π_x and R_y are generalized interpolation operators defined as

$$\Pi_x(q) = \sum_{i=1}^{4} \frac{\partial N_i}{\partial x} x_i q_i, \quad R_y(q) = \sum_{i=1}^{4} \frac{\partial N_i}{\partial x} y_i q_i \tag{21}$$

Here N_i denotes the standard isoparametric bilinear shape function which attains the value one at the node (x_i, y_i) and vanishes at the other nodes. Similar calculations show that

$$\bar{\beta}_{22} = \frac{\partial v}{\partial y} + \Pi_y\left(\frac{w}{R_{22}}\right) + \frac{R_x(w)}{R_{12}(0,0)} \tag{22}$$

and

$$\begin{aligned} \bar{\beta}_{12} = {} & \frac{1}{2}\left(\frac{\partial u}{\partial y} + \frac{\partial v}{\partial x} + \frac{\Pi_x w}{R_{12}(0,0)} + \frac{\Pi_y w}{R_{12}(0,0)}\right) \\ & + \frac{1}{2}\left[R_x\left(\frac{w}{R_{11}}\right) + R_y\left(\frac{w}{R_{22}}\right)\right] \end{aligned} \tag{23}$$

where

$$\Pi_y(q) = \sum_{i=1}^{4} \frac{\partial N_i}{\partial y} y_i q_i, \quad R_x(q) = \sum_{i=1}^{4} \frac{\partial N_i}{\partial y} x_i q_i \tag{24}$$

in analogy with (21).

We see that the above computed $\bar{\beta}_{11}$ and $\bar{\beta}_{22}$ agree with $\beta_{11,h}$ and $\beta_{22,h}$ obtained in (16) if the last terms were omitted from (20) and (22). However, by utilizing the additional terms involving R_x, R_y, it can be shown as in [12] that

$$\bar{\beta}_{11} = \bar{\beta}_{22} = 0 \quad \Rightarrow \quad \bar{\beta}_{12} = \beta_{12,h} + \mathcal{O}(h_K^2/R^2) \tag{25}$$

This means that when bilinear degenerated elements are used to approximate inextensional displacement modes, the underlying difference equations for the constraints $\beta_{ij} = 0$ are almost identical with those arising from the utilization

of (16). As a matter of fact, the above analysis provides a slight generalization of the original result in [12]. Namely, we did not assume that the element-wise defined geometric curvatures are constant parameters as in [12] where these were computed from a quadratic expansion of f in (8). It should be noted that the formal accuracy is not any better when the curvatures are derived from the interpolated normal vector $\tilde{\mathbf{n}}$ by using (10), but in order to keep the constraint ratio (15) at the optimal value, only one membrane constraint per each side of the mesh is allowed[8].

On the other hand, in the MITC4 element of Bathe & Dvorkin, the transverse shear strains are modified explicitly by using reduced strain techniques into the covariant strain components $\epsilon_{1z}, \epsilon_{2z}$. Using tensor transformation rules, it can be shown that the mixed interpolation of the tensorial components leads (approximatively, see [12]) to transverse shear strains of the form

$$\bar{\rho}_{1,h} = \Pi_x\theta - \frac{\partial w}{\partial x} + \Pi_x\left(\frac{u}{R_{11}}\right) + \Pi_x\left(\frac{v}{R_{12}}\right)$$
$$\bar{\rho}_{2,h} = \Pi_y\psi - \frac{\partial w}{\partial y} + \Pi_y\left(\frac{u}{R_{12}}\right) + \Pi_y\left(\frac{v}{R_{22}}\right)$$

which are readily in agreement with those obtained from (16). We note that the geometry approximation leads generally to a modification of the bending strains as well, see [12]. However, as the bending strains are not very prone to parametric effects, it seems that the numerical effect of this modification is rather marginal (although undesirable).

In the thesis, the above interpretation of the MITC4 shell element is referred to as MITC4F. We have seen that on rectangular meshes, the leading terms of the membrane and transverse shear strains of MITC4F and MITC4S are closely related, the chief difference being the additional terms in the expressions of the membrane strains of MITC4F. If K is of size $h_x \times h_y$, we have

$$R_x(q) \sim h_x\frac{\partial q}{\partial y}, \quad R_y(q) \sim h_y\frac{\partial q}{\partial x} \tag{26}$$

and

$$q - \Pi_x(q) \sim h_x\frac{\partial q}{\partial x}, \quad q - \Pi_y(q) \sim h_y\frac{\partial q}{\partial y} \tag{27}$$

so that the use of either element causes formally an effect of relative order $\mathcal{O}(h_K/L)$ to the relevant consistency error functional when the displacement field to be approximated is uniformly smooth with respect to t in the length scale L. However, the *anisotropic* character of the estimates (26) may change the situation rather dramatically if the displacement field varies in different length scales in different coordinate directions. To observe this, we let the length scales characterizing the deformation mode be L and H in the x- and y-direction, respectively, and assume that $L \ll H$. Then $R_y(w) \sim h_y/L$ by (26) so that if MITC4F is used, some terms in (17) may become amplified

[8]This is crucial also in practice if the computations are based on the refined shallow shell model and the curvatures of the shell are rapidly varying.

by the ratio of anisotropy $r = H/L \gg 1$ as compared with the approximation theoretically optimal order h_y/H. Note that anisotropically varying displacement modes are rather common among shell deformations in the form of boundary and interior layers but vibration modes arising in dynamical problems may also exhibit similar behavior, cf. [23].

In addition to the possibly harmful amplification of the consistency error functional, the energy formulation of layer and vibration problems may enforce membrane constraints that can be problematic for MITC4F. The reason for this lies in the fact that in order for $\bar{\beta}_{12}$ to reduce to the midpoint evaluation, $\bar{\beta}_{11}$ and $\bar{\beta}_{22}$ must vanish. Because this is not the case for layer and vibration modes (see [22, 23]), MITC4F may become over-constrained in their approximation.

In paper [C], a detailed error analysis is carried out concerning the approximation of *Fourier layer modes* of the form

$$\mathbf{u}(x, y) = \mathbf{U} \cos(ky) e^{-\lambda(t)x}$$

using different bilinear elements on rectangular grids. Here $H = k^{-1} = R$ is the (fixed) length scale of variation along the layer generator and $L = L(t) = 1/\mathrm{Re}\ \lambda(t)$ is the characteristic decay length scale of the layer mode such that $L(t) \to 0$ as $t \to 0$. Three possibilities were investigated where

$$L(t) = \begin{cases} \sqrt{Rt}, & \text{Case 1} \\ \sqrt[3]{R^2 t}, & \text{Case 2} \\ \sqrt[4]{R^3 t}, & \text{Case 3} \end{cases}$$

depending on the shell geometry. It was shown that when MITC4F is used, parametric locking arises as a rule. Namely, the derived a priori error estimates predict error magnification by factors R/L (Cases 1,3) and $(R/L)^2$ (Case 2) from the optimal convergence rate when the relative error is measured in the (modified) energy norm. The error amplification effect is also observed in numerical experiments.

A sceptical reader may have doubts about our simplified theory where certain small-looking terms are neglected while some other terms, which are formally of the same order, are kept. In order to assure the applicability of the theory, the thesis culminates in paper [E] where MITC4S is compared directly with the bilinear elements of the commercial codes ABAQUS and ADINA in benchmark tests involving layer and vibration modes. Moreover, the formulation of MITC4S in paper [E] is suitable for rather general (linear) shell analyses as it allows elements of arbitrary quadrilateral shape to be used and requires only the nodal positions and normals as geometric initial data.

This extended introduction for the thesis ends up with a practical example which should put things in perspective.

2.4 Case study: Vibration analysis of a fan blade

A shell problem of considerable practical importance is that of the vibration of curved fan blades. Such fan blades are quite common in jet engines powering aircraft around the globe. A cylindrical compressor blade depicted in Figure 2 serves as a representative example. Some time ago, Olson and Lindberg constructed an experimental model of this blade which was made of steel and built-in to a rigid foundation along the other curved edge as indicated in Figure 2. The vibration modes of the shell were then excited by a sinusoidal magnetic force and the first twelve vibration frequencies have been reported in [30] together with an initial finite elements analysis.

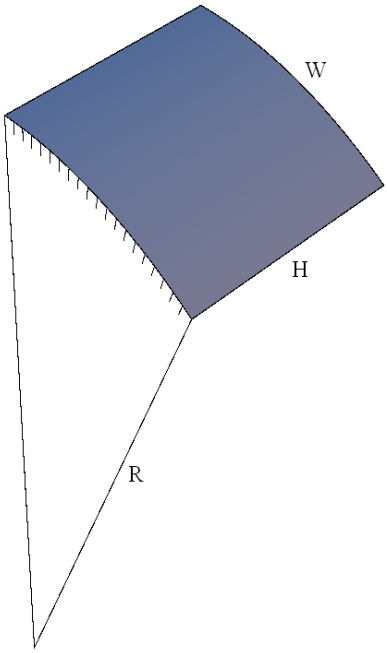

Properties of the blade:

Young modulus[9]:	$3 \cdot 10^7$ psi
Poisson ratio:	0.3
Mass density:	0.28 lb/in^3
Thickness:	0.12 in
Radius of curvature (R):	24 in
Developed width (W):	12 in
Height (H):	12 in

Figure 2: A cylindrical compressor blade made of steel.

Here we perform the finite element analysis by using two kinds of bilinear isoparametric representations of the blade as shown in Figure 3. Some of the lowest vibration frequencies (cycles per second) have been computed by using MITC4S as formulated in paper [E] and the original MITC4 element of ADINA together with its generalization MITC4IM, where the in-plane displacements are supplemented by the so-called incompatible displacement modes, cf. [29].

[9]It should be noted that the "gravitational" factor 32.17405 $(\mathrm{lb} \cdot \mathrm{ft})/(\mathrm{lb_f} \cdot \mathrm{s}^2)$ is required here to arrive at a coherent system of units.

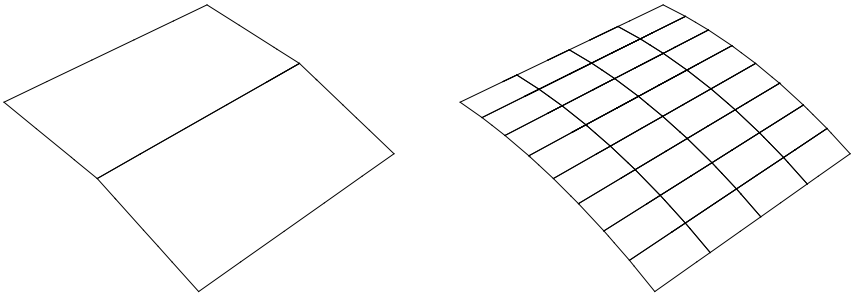

Figure 3: Two bilinear finite element models of the compressor blade.

The frequencies in Table 1 contrast sharply with laboratory test results which indicates that the mesh is too coarse. On the other hand, the few lowest frequencies in Table 2 are already in a rather good agreement with the experimental values. Note that the fundamental frequency, i.e. the lowest frequency, is approximated within the engineering accuracy of 2% by MITC4S whereas the error of MITC4 is about 8%. Our claim is that this occurs because the energy formulation of the corresponding vibration mode enforces the membrane constraints[10] $\beta_{22} = 0$ and $\beta_{12} = 0$, but not the constraint $\beta_{11} = 0$, see [23]. Consequently, the implication (25) is not disposable and MITC4 becomes slightly over-constrained via the constraint $\bar{\beta}_{12} = 0$. Apparently, the incompatible displacement modes in MITC4IM are able to relax this constraint.

Mode	MITC4S	MITC4	MITC4IM	[30]
1	66.3	68.6	68.6	86.6
2	157.7	125.5	112.3	135.5
3	261.4	481.3	380.5	258.9

Table 1: The vibration frequencies (Hz) of the first three modes: 1×2 mesh.

Mode	MITC4S	MITC4	MITC4IM	[30]
1	87.9	93.5	89.5	86.6
2	145.4	148.1	142.2	135.5
3	249.7	266.4	262.7	258.9
4	391.5	410.5	394.2	350.6
5	443.6	452.2	439.8	395.2
6	579.7	601.1	600.1	531.1
7	801.5	857.1	842.2	743.2

Table 2: The vibration frequencies (Hz) of the first seven modes: 4×8 mesh.

[10]Here 1 refers to the axial direction and 2 to the angular direction.

3 Concluding remarks

The main results of the thesis can be summarized as follows:

[A] The paper sheds light on both mechanical behavior of shells, particularly in view of concentrated point loads, and performance of corresponding finite element schemes. An honest comparison of standard *hp*-type finite elements and MITC4S is presented. The results confirm the robustness of high-order finite elements and show that the numerical modifications in MITC4S improve the standard bilinear scheme considerably also when approximating layers.

[B] The paper evaluates bilinear shell elements based on classical shell theory and 2D finite element framework. A couple of different formulations are presented and their accuracy is studied in membrane- and bending-dominated deformations. Although none of the studied formulations can be called as "locking-free" on a general quadrilateral mesh, it appears that on distorted meshes certain explicit reductions of the usual 2D membrane strains might work better than the implicit modifications arising from the use of bilinear degenerated 3D elements.

[C] The paper analyzes the effect of boundary and interior layers on the accuracy of the simplest quadrilateral shell elements with four nodes. The theoretical results predict that formulations, where the membrane strains are computed using the degenerated solid approach, suffer from parametric locking effects when capturing shell layers. In particular, the approximation of the characteristic layers in hyperbolic shells seems to be the most challenging task. On the other hand, the paper asserts that the optimal accuracy of bilinear finite elements can be maintained if the membrane strains are first computed locally as suggested by shallow shell theory and then modified carefully in order to avoid locking.

[D] The paper deals again with point loaded shell structures, both in theoretical and in numerical sense. The analysis and computations recall and extend the results of the full length paper [A] in view of the theory of paper [C]. Namely, a study of the fundamental solution of a shallow shell and corresponding finite element computations is presented. Firstly, the kinematics of the shell model is simplified by imposing the classical Kirchhoff-Love constraints. Secondly, the solution of the resulting Euler equations is given as a Fourier expansion for elliptic, hyperbolic and parabolic geometries. Then, the behavior of the solution, in particular the length scales of the characteristic line layers, are carefully analyzed and illustrated by contour plots in different cases. Finally, the approximation capability of finite elements is tested by comparing the *p*- and *h*-strategies. As the main result of the benchmarking, one can see the inferior capability of the *h*-strategy, which is based on an interpretation of the degenerated solid procedure, in resolving the line layer for the hyperbolic shell geometry.

[E] The final paper of the thesis pulls together the observations made in papers [A]–[D] and introduces a four-node shell element which is based on classical shell theory but should be applicable also to practical computations. The benchmark computations of the paper show that, in cases where shell layers or vibration modes are approximated on anisotropically refined meshes, the accuracy of the proposed formulation is indeed superior to that of the popular bilinear elements in commercial codes ABAQUS and ADINA.

References

[1] Belytschko T, Liu W, Moran B. *Nonlinear Finite Elements for Continua and Structures*. John Wiley & Sons Ltd.: Chichester, 2000.

[2] MacNeal RH. A simple quadrilateral shell element. *Comput. Struct.* 1978; **8**:175–183.

[3] Wempner G, Talaslidis D, Hwank CM. A simple and efficient approximation of shells via finite quadrilateral elements. *J. Appl. Mech.* 1982; **49**:115–120.

[4] Dvorkin EN, Bathe KJ. A continuum mechanics based four-node shell element for general non-linear analysis. *Eng. Comput.* 1984; **1**:77–88.

[5] Bathe KJ, Iosilevich A, Chapelle D. An evaluation of the MITC shell elements. *Comput. Struct.* 2000; **75**:1–30.

[6] Kikuchi F. On the validity of the finite element analysis of circular arches represented by an assemblage of beam elements. *Comput. Methods Appl. Mech. Engrg.* 1975; **5**:253–276.

[7] Chapelle D. A locking-free approximation of curved rods by straight beam elements. *Numer. Math.* 1997; **77**:299–322.

[8] Büchter N, Ramm E. Shell theory versus degeneration - a comparison in large rotation finite element analysis. *Int. J. Numer. Meth. Engng* 1992; **34**:39–59.

[9] Chapelle D, Bathe KJ. The mathematical shell model underlying general shell elements. *Int. J. Numer. Meth. Engng* 2000; **48**:289–313.

[10] Chapelle D, Bathe KJ. *The Finite Element Analysis of Shells: Fundamentals*. Springer: Germany, 2003.

[11] Malinen M. On the classical shell model underlying bilinear degenerated shell finite elements. *Int. J. Numer. Meth. Engng* 2001; **52**:389–416.

[12] Malinen M. On the classical shell model underlying bilinear degenerated shell finite elements: general shell geometry. *Int. J. Numer. Meth. Engng* 2002; **55**:629–652.

[13] Havu V, Pitkäranta J. Analysis of a bilinear finite element for shallow shells I: Approximation of inextensional deformations. *Math. Comp.* 2002; **71**:923–943.

[14] Havu V, Pitkäranta J. Analysis of a bilinear finite element for shallow shells II: Consistency error. *Math. Comp.* 2003; **72**:1635–1653.

[15] Pitkäranta J. The problem of membrane locking in finite element analysis of cylindrical shells. *Numer. Math.* 1992; **61**:523–542.

[16] Bathe KJ, Dvorkin EN. A four-node plate bending element based on Mindlin/Reissner plate theory and a mixed interpolation. *Int. J. Numer. Meth. Engng* 1985; **21**:367–383.

[17] Wlassow W. *Allgemeine Schalentheorie und ihre Anwendung in der Technik*. Akademie-Verlag: Berlin, 1958.

[18] Novozhilov VV. *The Theory of Thin Shells*. P. Noordhoff, Ltd. Groningen: The Netherlands, 1959.

[19] Gol'denveizer AL. *Theory of elastic thin shells*. Pergamon Press Ltd.: Great Britain, 1961. Trans.; orig. Russian vol.: Gostekhizdat, 1953.

[20] Flügge W. *Stresses in Shells*. Springer-Verlag: Germany, 1973.

[21] Lukasiewicz S. *Local loads in plates and shells*. Sijthoff & Noordhoff: The Netherlands, 1979.

[22] Pitkäranta J, Matache AM, Schwab C. Fourier mode analysis of layers in shallow shell deformations. *Comput. Methods Appl. Mech. Engrg.* 2001; **190**:2943–2975.

[23] L Beirão da Veiga, Hakula H, Pitkäranta J. Asymptotic and numerical analysis of the eigenvalue problem for a clamped cylindrical shell. *I.M.A.T.I.-C.N.R.* 2007; :1–17.

[24] Pitkäranta J, Leino Y, Ovaskainen O, Piila J. Shell deformation states and the finite element method: a benchmark study of cylindrical shells. *Comput. Methods Appl. Mech. Engrg.* 1995; **128**:81–121.

[25] Hughes TJR. *The Finite Element Method. Linear Static and Dynamic Finite Element Analysis*. Prentice-Hall: Englewood Cliffs, New Jersey, 1987.

[26] Strang G, Fix G. *An analysis of the finite element method*. Prentice-Hall, Inc.: Englewood Cliffs, N.J., 1973.

[27] Pitkäranta J. The first locking-free plane-elastic finite element: historia mathematica. *Comput. Methods Appl. Mech. Engrg.* 2000; **190**:1323–1366.

[28] Zienkiewicz O, Taylor R. *The finite element method. Volume 2: Solid mechanics. Fifth edition.* Butterworth-Heinemann: Oxford, 2000.

[29] Bathe KJ. *Finite Element Procedures.* Prentice Hall: Englewood Cliffs, 1996.

[30] Olson M, Lindberg G. Vibration analysis of cantilevered curved plates using a new cylindrical shell finite element. *AFFDL Report* 1968; **AFFDL-TR-68-150**:247–269.

(continued from the back cover)

A558 José Igor Morlanes, Antti Rasila, Tommi Sottinen
Empirical evidence on arbitrage by changing the stock exchange
December 2008

A556 Lourenço Beirão da Veiga, Jarkko Niiranen, Rolf Stenberg
A posteriori error analysis for the Morley plate element with general boundary conditions
December 2008

A555 Juho Könnö, Rolf Stenberg
Finite element analysis of composite plates with an application to the paper cockling problem
December 2008

A554 Lasse Leskelä
Stochastic relations of random variables and processes
October 2008

A553 Rolf Stenberg
A nonstandard mixed finite element family
September 2008

A552 Janos Karatson, Sergey Korotov
A discrete maximum principle in Hilbert space with applications to nonlinear cooperative elliptic systems
August 2008

A551 István Faragó, Janos Karatson, Sergey Korotov
Discrete maximum principles for the FEM solution of some nonlinear parabolic problems
August 2008

A550 István Faragó, Róbert Horváth, Sergey Korotov
Discrete maximum principles for FE solutions of nonstationary diffusion-reaction problems with mixed boundary conditions
August 2008

A549 Antti Hannukainen, Sergey Korotov, Tomás Vejchodský
On weakening conditions for discrete maximum principles for linear finite element schemes
August 2008

HELSINKI UNIVERSITY OF TECHNOLOGY INSTITUTE OF MATHEMATICS
RESEARCH REPORTS

The reports are available at *http://math.tkk.fi/reports/* .
The list of reports is continued inside the back cover.

A563 Dmitri Kuzmin, Sergey Korotov
Goal-oriented a posteriori error estimates for transport problems
February 2009

A562 Antti H. Niemi
A bilinear shell element based on a refined shallow shell model
December 2008

A561 Antti Hannukainen, Sergey Korotov, Michal Krizek
On nodal superconvergence in 3D by averaging piecewise linear, bilinear, and trilinear FE approximations
December 2008

A560 Sampsa Pursiainen
Computational methods in electromagnetic biomedical inverse problems
November 2008

A559 Sergey Korotov, Michal Krizek, Jakub Solc
On a discrete maximum principle for linear FE solutions of elliptic problems with a nondiagonal coefficient matrix
November 2008

ISBN 978-951-22-9783-2 (print)
ISBN 978-951-22-9784-9 (PDF)
ISSN 0784-3143 (print)
ISSN 1797-5867 (PDF)
Multiprint Oy
Espoo 2009